scientific reports

Check for updates

OPEN

Isoimperatorin improves osteoporosis by increasing YBX1 expression to promote BGLAP m5C modification

Guang Hu[1], Jing Wen[2], Hao Yang[3] & Kaiwei Zhang[1,3]✉

Osteoporosis is a chronic metabolic bone disease that is prone to fractures. Isoimperatorin (ISO) has been shown to alleviate the bone loss in ovariectomized (OVX) rats. The aim of this study was to investigate the effect and the mechanism of ISO on osteoporosis using animal study and cell experiments. Osteogenic differentiation was assessed by alkaline phosphatase activity detection, and alizarin red S staining. The expression of osteogenic differentiation-related genes and m5C regulators was measured using quantitative real-time PCR. Hematoxylin eosin (H&E) staining and microCT were performed to evaluate osteoporosis in vivo. The m5C levels in mice were measured by dot blot assay, and the binding between ISO and YBX1 was assessed by biolayer interferometry (BLI) analysis and molecular docking. Methylated RNA immunoprecipitation was performed to identify the target gene of YBX1. The interaction between YBX1 and BGLAP was assessed using RIP and luciferase reporter assay. Results suggested that ISO significantly promoted osteogenic differentiation of MC3T3 cells and alleviated osteoporosis in OVX mice. Moreover, ISO increased m5C level and YBX1 expression in OVX mice, while YBX1 knockdown inhibited osteogenic differentiation in ISO-treated MC3T3 cells, and restored osteoporosis in OVX mice ameliorated by ISO. Additionally, YBX1 knockdown inhibited the m5C level of BGLAP through inhibiting its mRNA stability. In conclusion, we demonstrated that ISO improved osteoporosis through increasing YBX1 expression thereby upregulating the m5C modification of BGLAP. These results may provide a novel theoretical basis for ISO treatment of osteoporosis.

Keywords Osteoporosis, Isoimperatorin, m5C modification, YBX1, BGLAP, Osteogenic differentiation

Osteoporosis is a chronic metabolic bone disease that includes primary osteoporosis caused by menopause and old age, and secondary osteoporosis caused by a variety of diseases[1,2]. Cell differentiation of osteoporosis is altered, with the inhibition of osteogenic differentiation and the increase of adipogenic differentiation[3]. Due to the ageing population in many countries, the prevalence of osteoporosis is increasing in recent years, seriously affecting the quality of life of patients[4]. Osteoporosis is characterized by low bone density and is prone to fractures due to decreased bone mass, excessive bone loss and destruction of bone structure[5]. Therefore, prevention of fracture is the main goal in the treatment of osteoporosis. The drugs currently used to treat osteoporosis can be divided into two categories: bone resorption inhibitors, which increase mineralisation through inhibiting osteoclastogenesis, and bone formation enhancers[6]. Despite current developments in drug therapy for osteoporosis, side effects such as osteonecrosis of the jaw still exist. Therefore, continued development of new treatments for osteoporosis is necessary.

Isoimperatorin (ISO) is a group of active substances found in a wide range of medicinal plants, including Angelica dahurica and Adenophora japonica. ISO has a variety of phrmacological effects, including anti-inflammatory, antioxidant, and modulation of apoptosis, and is a potent antiviral and antitumour agent[7–11]. Recently, a study revealed that ISO alleviates the bone loss in ovariectomized (OVX) rats, suggesting that ISO may be an effective therapeutic drug for osteoporosis[12]. However, the mechanism of ISO in the treatment of osteoporosis is still insufficient.

[1]The First Affiliated Hospital of Guizhou University of Traditional Chinese Medicine, Guiyang 550001, Guizhou, China. [2]The Affiliated Hospital of Guizhou Medical University, Guiyang 550004, Guizhou, China. [3]Guizhou University of Traditional Chinese Medicine, No. 71, North Baoshan Road, Yunyan District, Guiyang 550025, Guizhou, China. ✉email: kaiweizhang11@outlook.com

RNA modifications play a key regulatory role in cell biology by affecting processes such as RNA production, transport and metabolism. 5-methylcytosine (m5C) is a widely prevalent RNA modification, which is widely distributed in both mRNAs and non-coding RNAs, including tRNA, rRNA, snRNA and eRNA[13]. m5C affects the expression of downstream target genes by influencing the stability and translation of different RNAs to perform different biological functions[14]. m5C is mediated by three types of proteins: methyltransferase (writer), demethylase (eraser), and reading protein (reader). Among them, the NSUN family and TRDMT1 were identified as writers, while the ALKBH1 and TET families belong to the erasers, and ALYREF and YBX1 mainly act as m5C readers[15,16]. m5C is involved in the pathogenesis of multiple diseases, including cancers, autoimmune disease and diabetes[17–19]. A study recently reported that m5C modification mediates the development of osteoporosis, and YBX1 deletion inhibits osteogenic differentiation of bone mesenchymal stromal cells in a m5C-dependent manner[20]. However, whether m5C mediates osteoporosis through regulating m5C modification remain unclear.

In this study, we investigated the effect of ISO on osteoporosis, and explored the mechanism by which ISO improves osteoporosis through m5C modification through animal study and cell experiments. This study may provide a theoretical basis for the application of ISO in the treatment of osteoporosis.

Methods

Animal study

Eight-week-old female wild-type C57BL/6 mice were housed at a 12 h light/dark cycle condition at 23–25 ℃ with free access to food and water. The mice were randomly divided into eight groups: the Sham + Vehicle group, Sham + ISO (5 mg/kg) group, Sham + ISO (10 mg/kg) group, Sham + Vehicle + Lv-shNC group, Sham + ISO (10 mg/kg) + Lv-shNC group, Sham + ISO (10 mg/kg) + Lv-shYBX1 group, OVX + Vehicle group, OVX + ISO (5 mg/kg) group, OVX + ISO (10 mg/kg) group, OVX + Vehicle + Lv-shNC group, OVX + ISO (10 mg/kg) + KO-NC group and OVX + ISO (10 mg/kg) + KO-YBX1 group, with six mice each group.

To establish the osteoporosis mouse model, mice were anesthetized by 0.1% pentobarbital sodium and both ovaries were excised under sterile conditions in the OVX group. Part of the fat tissue around the ovaries of mice in the sham group was removed. To investigate the effect of ISO, mice in the ISO treatment group were given oral ISO (5 mg/kg or 10 mg/kg) one week after ovariectomy. Other groups of mice received the same volume of phosphate buffer saline (PBS; Gibco, Grand Island, NY, USA) orally. ISO and PBS treatments were administered once daily for a total duration of 8 weeks[12]. To verify the function of YBX1, lentiviral containing short hairpin negative control (sh-NC) and short hairpin RNA YBX1 (sh-YBX1) were injected into the mice through the tail vein one day before ISO or PBS treatment. Ten weeks after ovariectomy, ISO treatment was completed and all mice were weighed, anesthetized, taken blood by enucleation of the eyeball, and then sacrificed by cervical dislocation. Femurs of mice were collected for the subsequent measurement.

Hematoxylin eosin (H&E) staining

The femurs of mice were stained with an HE staining kit (Beyotime, Beijing, China). Femurs were fixed with 10% paraformaldehyde, paraffin embedded, cut into 5 μm thick sections, and stained with hematoxylin and eosin according to the manufacturer's protocol and observed under a light microscope. Osteoblast surface per bone surface (Ob.S./BS) was quantified by Image J software.

Dynamic histomorphometry

Bone formation rate per bone surface (BFR/BS) was evaluated by dynamic histomorphometry. Mice were intraperitoneally injected with calcein (10 mg/kg) 10 days before sacrifice and alizarin red (30 mg/kg) 3 days before sacrifice to label newly formed bone regions. After mice were sacrificed, femurs were collected, fixed in 4% paraformaldehyde, dehydrated, embedded in methyl methacrylate and made into 5 μm of sections. The sections were observed under a fluorescence microscope.

Tartrate-resistant acid phosphatase (TRAP) staining

TRAP was performed to evaluate osteoclastic differentiation of femurs in mice. The paraffin sections were stained with TRAP staining solution (Jiancheng Bioengineering Institute, Nanjing, China) according to the manufacturer's protocol. The results were observed under a microscope and analyzed by Image J software.

MicroCT

After euthanasia, the right femur of each mouse was isolated, fixed in 10% neutrally buffered formalin for 2 d, and then transferred to 70% ethanol. Bones were scanned using a μ-CT (SkyScan, Kontich, Belgium) at 50 kV, 120 mA and 10 μm voxel resolution. Measurement indicators include bone mineral density (BMD), trabecular bone volume fraction (BV/TV), trabecular number (Tb.N), bone Volume (BV), trabecular separation/spacing (Tp.Sp), bone surface (BS).

Cell culture and treatment

Mouse precranial osteoblast cell line MC3T3 cells were provided from Cell Bank of the Chinese Academy of Sciences (Shanghai, China) and cultured in α-minimum essential medium (α-MEM; Gibco) supplement with 10% fetal bovine serum (FBS; Gibco) in a humidity incubator at 37℃ with 5% CO_2. The chemical structure of ISO is shown in Fig. 1A. To assess the effect of ISO on MC3T3 cells, cells were treated with 0, 2.5, 5 and 10 μM of ISO (MedChem Express, Monmouth Junction, NJ, USA) for 24 h. To induce osteogenic differentiation, cells were cultured in α-MEM supplement with 10% FBS, 10 mM β-glycerol phosphate and 50 μg/ml ascorbic acid for 14 d.

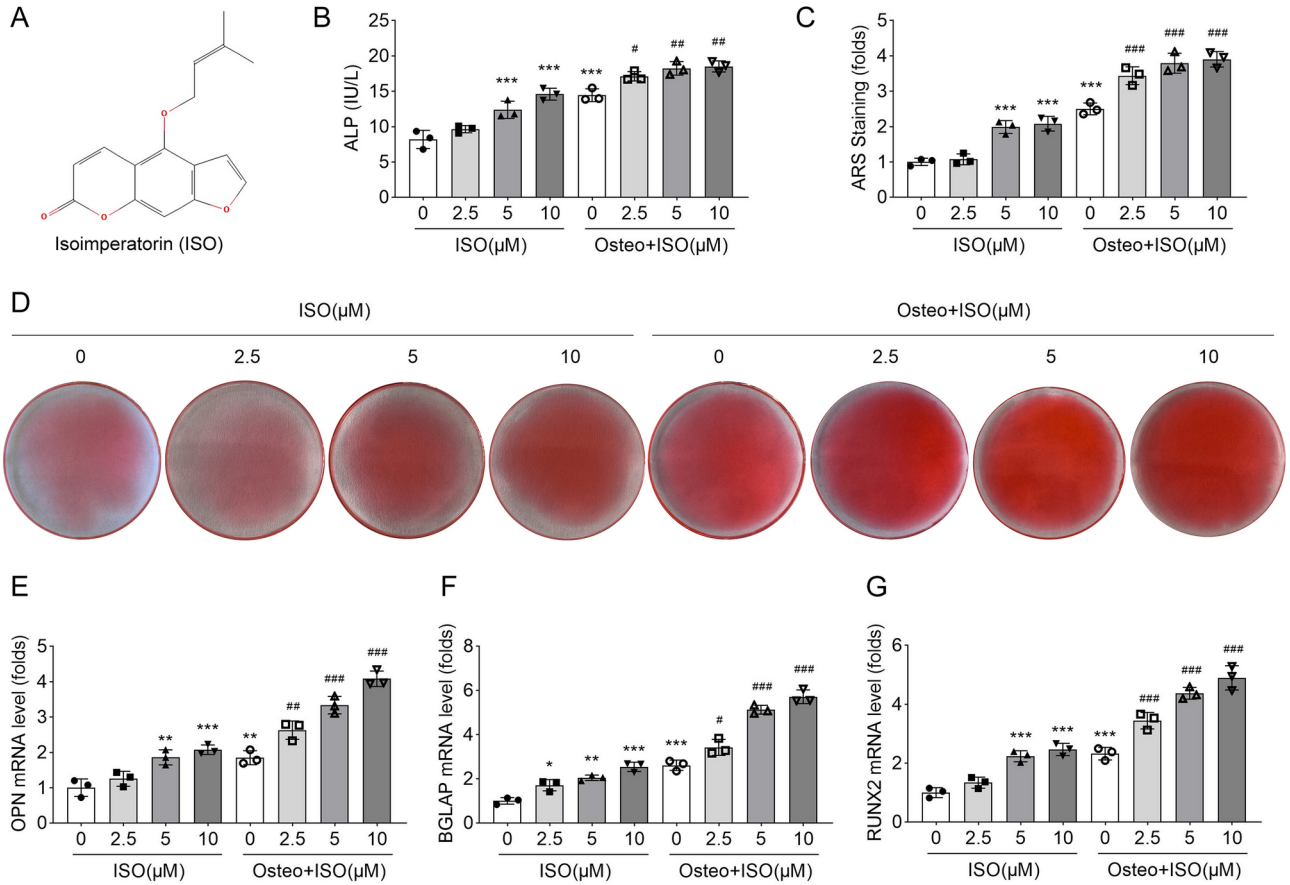

Fig. 1. ISO promoted osteogenic differentiation of MC3T3 cells. (**A**) The chemical structure of ISO. (**B**) The ALP activity was measured using an ALP assay kit. (**C** and **D**) An ARS staining kit was performed to assess the osteoblast mineralization nodules. (**E**–**G**) The expression of OPN, BGLAP and RUNX2 was measured by qPCR. **P < 0.01 and ***P < 0.001 vs. the 0 μM group without osteogenic induction. #P < 0.05, ##P < 0.01 and ###P < 0.001 vs. the 0 μM group with osteogenic induction.

Cell transfection

Short hairpin RNA targeting YBX1 (sh-YBX1) and shRNA negative control (sh-NC) were provided from GenePharma (Shanghai, China). These sequences were transfected into MC3T3 cells using Lipofectamine 2000 (Invitrogen, Carlsbad, CA, USA) according to the manufacturer's protocol. The cells were harvested after 48 h transfection.

Alkaline phosphatase (ALP) activity detection

ALP activity was measured after osteogenic induction for 14 d using an ALP assay kit (Beyotime). The ALP activity was measured according to the manufacturer's protocol. The absorbance was measured at 405 nm.

Alizarin Red S (ARS) staining

After osteogenic induction for 14 d, cells were stained with ARS staining solution (Beyotime) for 30 min and observed using a microscope.

Quantitative real-time PCR (qPCR)

Total RNA was isolated using Trizol reagent (Thermo Scientific, Waltham, MA, USA). Then, RNA was reverse-transcribed into cDNA using a 1st Strand cDNA synthesis kit (Yeasen, Shanghai, China). qPCR was performed using SYBR green mix (Vazyme, Nanjing, China) on an Applied Biosystems (Thermo Scientific). Relative mRNA expression was calculated using the $2^{-\Delta\Delta Ct}$ method as normalized to GAPDH. The primers are shown in Table 1.

Dot blot assay

Extracted RNA was loaded on Hybond-N + membranes (Solarbio, Beijing, China) for 60 s of crosslink at 254 nm. Then, the membranes were blocked with 5% defatted milk for 1.5 h at room temperature, and then incubated with anti-m5C overnight at 4 °C and secondary antibodies for 1.5 h. Finally, the blots were visualized using an enhanced chemiluminescence kit (Thermo Scientific, Waltham, MA, USA).

Gene	Forward	Reverse
OPN	ATCTCACCATTCGGATGAGTCT	TGTAGGGACGATTGGAGTGAAA
BGLAP	ACCATCTTTCTGCTCACTCTGCT	CCTTATTGCCCTCCTGCTTG
RUNX2	GACTGTGGTTACCGTCATGGC	ACTTGGTTTTTCATAACAGCGGA
NOP2	CGAAAGGCCCGAAAACAGAAG	TGGATAACTCTCCAGGCAATGT
NSUN2	AGGTGGCTATCCCGAGATCG	GACTCCATGAATTGGTCCCATT
NSUN3	GACTCCATGAATTGGTCCCATT	AGGACTGTGTGATAGCCCCTC
NSUN4	AGGACTGTGTGATAGCCCCTC	AAGCATCGAAGATTTGGGCTG
NSUN5	ACCTGAAGCAGTTGTACGCTC	CCCCTTCCCCAGCAATAATTC
NSUN6	AAGACAACAGGGTGAAGTGATTG	TCCATCAAATTCTTTGGCTCCTT
NSUN7	TCTCAAGGTGGTCTACCGAAA	TTCATTGCGTGTGTTAGCTGT
TRDMT1	GCGCTGCGAGAAAGTCATATC	CCCTGTAGGCCAATTCTTGTG
ALYREF	GGCACCGTACAGTAGACCG	AAGTCCAGGTTTGACACGAGC
YBX1	AAGGTCATCGCAACGAAGGTT	CAAATACGTCTTCCTTGGTGTCA
ALKBH1	TGAACCTGTGAGCAAGTGGAG	GAGGAAGGGGTTTGGAATGAAAA
TET1	GCAGTGAACCCCGGAAAAC	AGAGCCATTGTAAACCCGTTG
TET2	CTCCCATCAGCCATACAGAACC	CTGACTGTGCGTTTTATCCCT
TET3	TGCGATTGTGTCGAACAAATAGT	TCCATACCGATCCTCCATGAG
RUNX1	GACTCACCTGTGGATGTGAAG	GACTCACCTGTGGATGTGAAG
Osx	GGAAAGGAGGCACAAAGAAGC	GGAAAGGAGGCACAAAGAAGC
ON	TGGGAGAATTTGAGGACGGTG	TGGGAGAATTTGAGGACGGTG
COL1A1	GCTCCTCTTAGGGGCCACT	ATTGGGGACCCTTAGGCCAT
OPG	CCTTGCCCTGACCACTCTTAT	CACACACTCGGTTGTGGGT
BMP2	GGCCGAAGGTGGATTCTCC	GTCGGGTGTGTTATTGACATACA
BMP7	CCTGTCCATCTTAGGGTTGCC	CCTGTCCATCTTAGGGTTGCC

Table 1. qPCR primers.

Biolayer interferometry (BLI) analysis

The interaction between YBX1 and ISO was identified using Octet RED 96 (ForteBio, Fremont, CA, USA). The Ni–NTA sensor was infiltrated using PBS for 10 min. ISO was diluted, and then dissolved in the machine. After the program, the results were analyzed using the ForteBio7.0 data analysis software.

Molecular docking

The chemical structures of the ISO were obtained from the PubChem database and were formatted and energy-minimised using Chem3D, and then imported into Schrodinger software for hydrogenation, structure optimisation, and energy-minimisation. The protein structure of YBX1 was obtained from the RCSB database and processed in the Maestro11.9 platform to optimise its geometry. Finally, molecular docking was performed with the Glide module in the Schrödinger Maestro software.

Methylated RNA immunoprecipitation (MeRIP)

The m5C levels of osteogenic differentiation-related genes were measured using a GenSeq m5C MeRIP kit (Cloudseq, Shanghai, China). Total RNA from MC3T3 cells was isolated using Trizol reagent, and was fragmented using the fragmentation buffer. Beads were pre-incubated with m5C antibody for 1 h, and then incubated with fragmented RNA for 1 h at 4 °C. Next, the beads were collected and purified and the m5C levels were measured by qPCR.

RIP

The interaction between YBX1 and BGLAP was evaluated using an imprint RIP kit (Sigma-Aldrich, St. Louis, MO, USA). MC3T3 cells were lysed in RIP lysis buffer. Then, the lysate was incubated with the anti-YBX1 or anti-IgG coated magnetic protein A/G beads overnight at 4 °C. The expression of BGLAP was detected by qPCR after purification.

Bioinformatic analysis

The m5C sites in BGLAP were predicted using the RNAm5Cfinder database (http://www.rnanut.net/rnam5cfinder/).

Dual luciferase reports

The combination of YBX1 and the potential m5C modification sites on BGLAP was assessed by dual luciferase reports. Mutant (mut)-BGLAP and wild-type (wt)-BGLAP contained site1 or site2 sequences were constructed. Cells were seeded into 96-well plates; when the cell fusion reaches 50–70%, cells were co-transfected with the

plasmids using Lipofectamine 2000 for 24 h. The luciferase activity was detected using a dual-luciferase reporter assay system (Promega, San Luis Obispo, CA, USA).

RNA stability assay

qPCR was performed to assess stability BGLAP mRNA after MC3T3 cells were treated with 5 μg/mL actinomycin D (Merck, Darmstadt, Germany) for 0, 2, 4, 8 and 12 h.

Statistical analysis

All data were expressed as mean ± standard deviation of at least three replicates and analyzed using SPSS 22.0 software. The comparison between two or more groups was performed by student's t-test or one-way analysis of variance (ANOVA). $P < 0.05$ was recognized as statistically significant.

Results

ISO promotes osteogenic differentiation of MC3T3 cells

To investigate the effect of ISO on osteoporosis, mouse precranial osteoblast cell line MC3T3 cells were treated with different concentrations of ISO to determine the effect of ISO on osteogenic differentiation and to screen the optimal concentration of ISO treatment. MC3T3 were cultured in α-MEM supplemented with osteogenic medium or not, respectively, and osteogenic differentiation was evaluated by detection of ALP activity and ARS staining. Results showed that ALP activity and osteoblast mineralization nodules gradually increased with the elevation of ISO treatment concentration, and 5 and 10 μM had the most significant enhancement effect; moreover, compared to MC3T3 cells without osteogenic induction, those subjected to osteogenic induction exhibited higher ALP activity and mineralized nodule formation (Fig. 1B–D). Additionally, we measured the expression of several osteogenic differentiation-related genes, OPN, BGLAP and RUNX2. Results showed that the expression of these genes was all significantly upregulated by ISO, while the increase was most significant after 5 and 10 μM of ISO treatment; moreover, the increase was more significant after osteogenic induction (Fig. 1E–G). In conclusion, we demonstrated that ISO promoted osteogenic differentiation of MC3T3 cells, and 5 and 10 μM had a better effect. However, although both 5 μM and 10 μM concentrations showed good effects in promoting osteogenic differentiation, there was no significant difference between the two concentrations. Therefore, we chose 5 μM for the subsequent experiments.

ISO attenuates the osteoporosis in OVX-induced mice

Next, OVX-induced mice were received 8-week ISO treatment to evaluate the effect of ISO on osteoporosis in vivo. H&E staining was performed to evaluate the pathological change of femur in mice. Results showed that the trabecular bone in both the sham group treated with ISO and the sham group without ISO treatment was evenly distributed and tightly arranged; compared to the sham group, the OVX group exhibited a reduced number of trabecular bones, uneven distribution, and sparse arrangement, indicating the development of osteoporosis in OVX-induced mice; ISO treatment increased the number and thickness of trabecular bones in OVX-induced mice, and the improvement at 10 mg/kg was superior to that at 5 mg/kg (Fig. 2A). TRAP was performed to evaluate osteoclast numbers in femur of mice. Compared to the sham group, the OVX group exhibited an increase in osteoclast number and positive area, and it was not affected by ISO treatment (Fig. 2A). Subsequently, microCT was performed to assess the bone structure of femur. Results showed that there was no significant difference in BMD, BV/TV, Tb.N, BV, Tb.Sp and BS between mice in the sham group received ISO treatment or not; BMD, BV/TV, Tb.N, BV and BS were all significantly decreased but Tb.Sp was elevated in the OVX mice, and these effects were enhanced by both 5 mg/kg and 10 mg/kg ISO treatment, and the effect of 10 mg/kg ISO was more significant (Fig. 2B–G). Moreover, there was no significance of BFR/BS and Ob.S./BS in the sham group received ISO treatment or not; compared with the sham group, BFR/BS and Ob.S./BS in OVX mice were significantly decreased, which was markedly elevated by ISO treatment in a dose dependent manner (Fig. 2H and I). Moreover, Oc.S./BS was elevated in the OVX mice, which was not affected by ISO treatment, indicating that ISO not affected osteoclastic differentiation in OVX mice (Fig. 2J). These results indicated that both 5 and 10 mg/kg of ISO treatment attenuated osteoporosis in OVX-induced mice, and the effects of 10 mg/kg were most significant. Therefore, 10 mg/kg of ISO was selected for the subsequent in vivo experiments.

ISO promotes m5C modification and YBX1 expression in the osteoporosis mouse model

To explore whether ISO affects the m5C modification of OVX-induced osteoporosis mouse model, we detected the m5C levels in femur tissues of the OVX-induced mice with 10 mg/kg ISO treatment or not. Dot blot suggested that the m5C levels of the ISO group was increased compared to that in the vehicle group (Fig. 3A). Next, we measured the mRNA levels of m5C-related genes in mice, and found that the expression of NSUN6 and YBX1 was markedly elevated in OVX-induced mice with 10 mg/kg of ISO treatment, and the increase of YBX1 expression was more significant (Fig. 3B, C). BLI analysis showed that the luminescence intensity of YBX1 increased with the elevation of ISO concentration, indicating that the expression level of YBX1 also increased with higher ISO concentrations (Fig. 3D). In addition, molecular docking results suggest that ISO can effectively bind to the active site of the YBX1 protein, indicating the combination of ISO and YBX1 (Fig. 3E). In conclusion, we demonstrated that ISO promoted m5C modification and YBX1 expression in the osteoporosis mouse model.

YBX1 knockdown inhibits osteogenic differentiation in ISO-treated MC3T3 cells

Next, the function of YBX1 in osteogenic differentiation was verified through in vitro experiments. qPCR suggested that YBX1 expression was significantly decreased after transfection with sh-YBX1 plasmids (Fig. 4A). Then, we assessed osteogenic differentiation in MC3T3 cells. Results showed that the ALP activity and ARS staining density elevated by 5 μM ISO in MC3TC cells with osteogenic induction or not was significantly

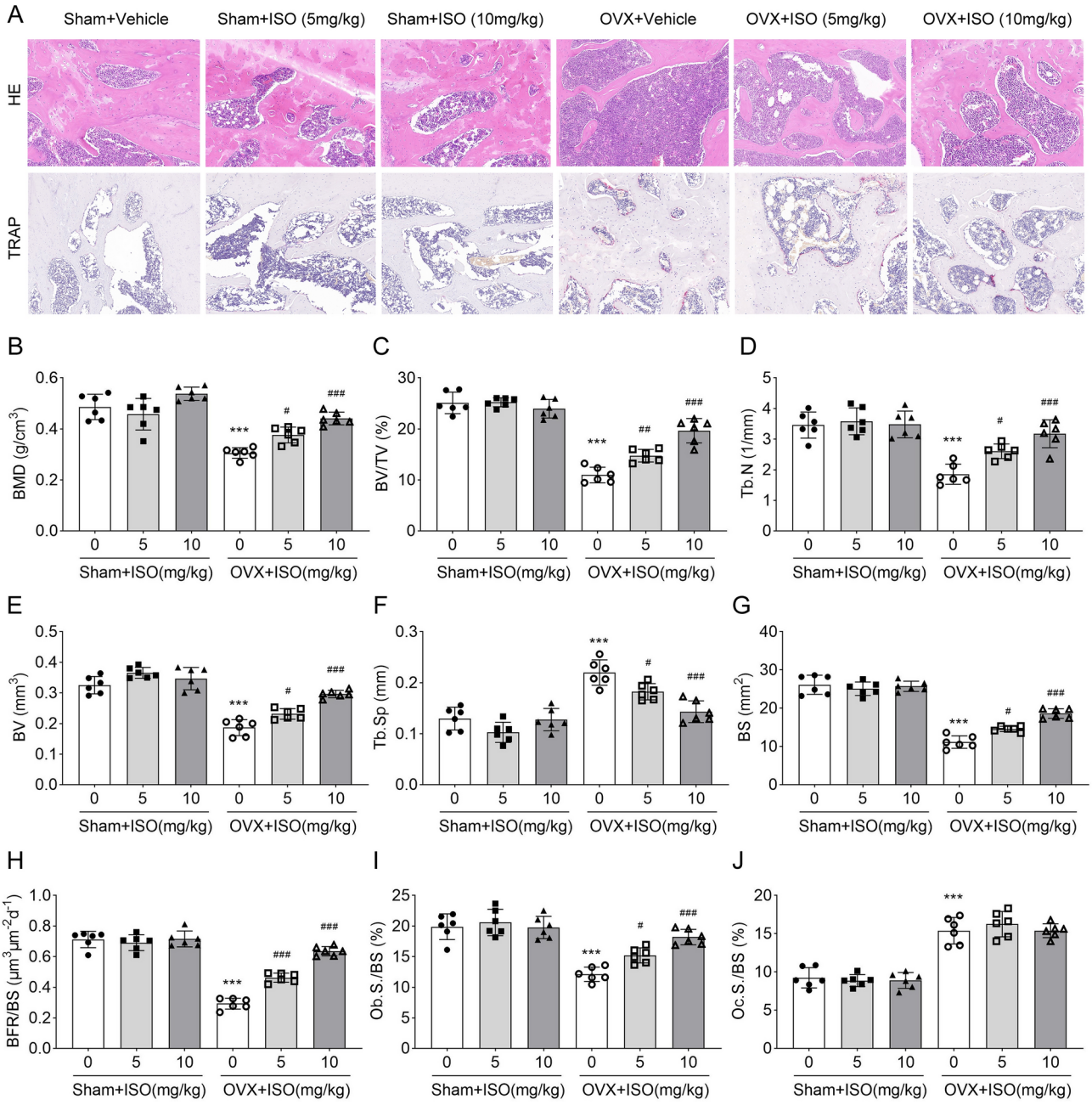

Fig. 2. ISO attenuated osteoporosis in OVX-induced mice. (**A**) The pathological change and osteoclastic differentiation of different group mice was assessed by H&E and TRAP staining. (**B**–**G**) BMD, BV/TV, Tb.N, BV, Tp.Sp and BS were detected by microCT. (**H**) BFR/BS was measured by dynamic histomorphometry. (**I**) Ob.S./BS was evaluated by H&E staining (**J**) Oc.S./BS were evaluated by TRAS staining. ***P < 0.001 vs. the sham + vehicle group. #P < 0.05, ##P < 0.01 and ###P < 0.001 vs. the OVX + Vehicle group.

decreased by YBX1 knockdown (Fig. 4B–D), indicating that 5 μM ISO enhanced osteogenic differentiation in MC3T3 cells, which was inhibited by YBX1 knockdown. Additionally, we measured the expression of several osteogenic differentiation-related genes in MC3T3 cells. Results suggested that ISO treatment significantly upregulated the expression of OPN, BGLAP and RUNX2 mRNA in ISO-treated MC3T3 cells with or without osteogenic induction, which was partially reversed by YBX1 knockdown (Fig. 4E–G). Moreover, osteogenic differentiation in MC3T3 cells was enhanced by osteogenic induction. Taken together, we demonstrated that YBX1 knockdown significantly inhibited osteogenic differentiation in ISO-treated MC3T3 cells.

YBX1 knockdown reverses the osteoporosis in OVX-induced mice alleviated by ISO

Next, sham operated mice or OVX-induced osteoporosis mice treated with vehicle or 10 mg/kg ISO treatment were transfected with YBX1 knockdown plasmids or its negative control to clarify the role of YBX1 in osteoporosis

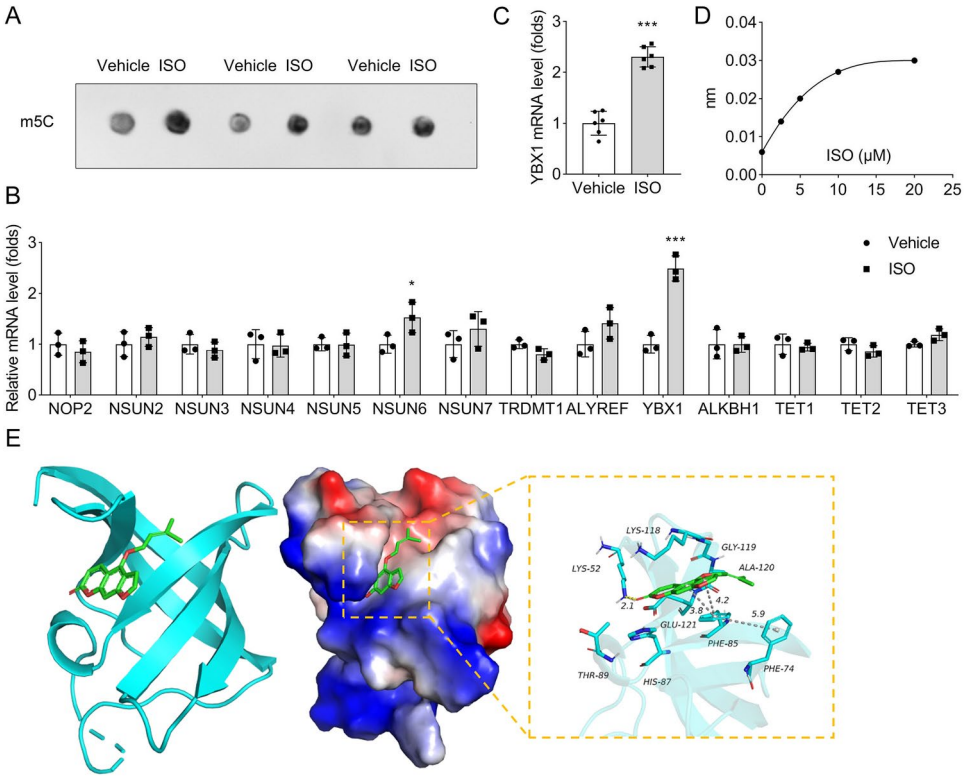

Fig. 3. ISO promoted m5C modification and YBX1 expression in the osteoporosis mouse model. (A) The m5C levels of femur tissues were measured by dot blot assay. The expression of (B) m5C regulators and (C) YBX1 mRNA in femur tissues of mice was assessed by qPCR. (D) BLI analysis was performed to identify the binding of ISO and YBX1. (E) Molecular docking showed the combination between ISO and YBX1. *P < 0.05 and ***P < 0.001 vs. The Vehicle group.

in vivo. H&E staining showed that the distribution of bone trabeculae was uneven and the arrangement was sparse in sham operated mice with YBX1 knockdown administrated ISO, indicating that YBX1 knockdown caused pathological damage to the femurs, but the damage was not serious due to ISO treatment; moreover, the pathological changes in the femurs of OVX-induced mice were partially improved by ISO treatment, but further aggravated by YBX1 knockdown (Fig. 5A). Moreover, TRAP staining suggested that the number of osteoclasts was increased in the OVX mice; notably, either YBX1 knockdown or ISO treatment affected osteoclast number in the sham group or the OVX group (Fig. 5A). Additionally, BMD, BV/TV, Tb.N, BV, BS, BFR/BS and Ob.S./BS in OVX-induced osteoporosis mice were significantly decreased compared to sham operated mice, but Tb.Sp was elevated; ISO treatment not affected these indicator in sham operated mice, but increased the levels of BMD, BV/TV, Tb.N, BV, BS, BFR/BS and Ob.S./BS and decreased Tb. Sp in OVX-induced mice, while these effects were reversed by YBX1 knockdown, indicating that YBX1 knockdown restored osteoporosis alleviated by ISO treatment (Fig. 5B–I). Moreover, compared to the sham group, Oc.S./BS was increased in the OVX mice, and ISO treatment and YBX1 knockdown not affected its value in the OVX mice (Fig. 5J). In conclusion, we demonstrated that YBX1 knockdown reversed the osteoporosis alleviated by ISO in OVX-induced mice.

YBX1 knockdown decreases the m5C level of BGLAP

To identify the target gene of YBX1, we measured the m5C levels of several osteogenic differentiation-related genes, and found that only the m5C level of BGLAP was significantly decreased by YBX1 knockdown (Fig. 6A). RIP assay suggested that there was an interaction between YBX1 and BGLAP (Fig. 6B). Next, we predicted two potential m5C modification sites of BGLAP, located at sites 60 and 306 of the BGLAP mRNA reference sequence (Fig. 6C), and dual luciferase report was performed to verify which site was modified by m5C. Results showed that YBX1 knockdown only inhibited the luciferase activity of WT-site1, but not affected the luciferase activity of WT-site2 (Fig. 6D). Additionally, YBX1 knockdown markedly accelerated the degradation of BGLAP, indicating that YBX1 knockdown inhibited the mRNA stability of BGLAP (Fig. 6E). Moreover, YBX1 knockdown downregulated the protein level of BGLAP in MC3T3 cells (Fig. 6F). Taken together, we demonstrated that YBX1 knockdown inhibited the m5C level and mRNA stability of BGLAP.

Discussion

Osteoporosis is a chronic metabolic bone disease that is common in older people and postmenopausal woman[21]. Patients with osteoporosis exhibit reduced bone mineral density and impaired bone microstructure, significantly increasing their risk of fractures. Osteogenic differentiation is the key to bone formation, and numerous studies

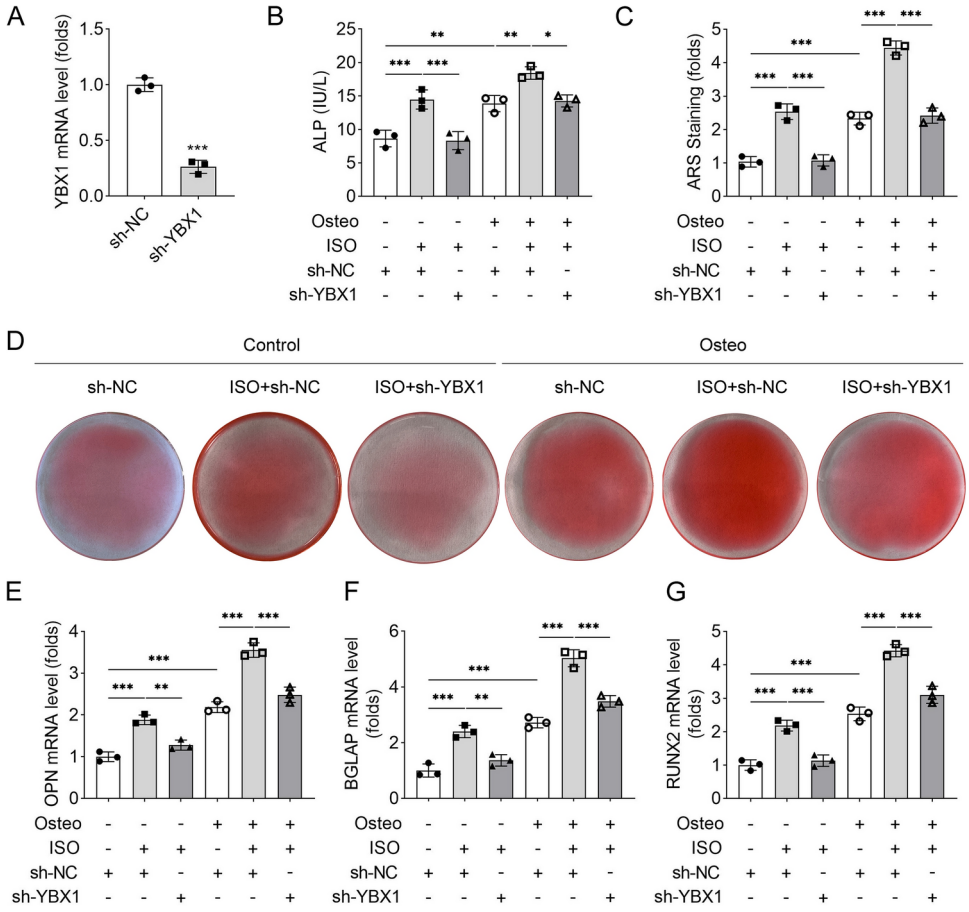

Fig. 4. YBX1 knockdown inhibited osteogenic differentiation in ISO-treated MC3T3 cells. (**A**) qPCR was performed to measure the expression of YBX1. (**B**) The ALP activity was measured using an ALP assay kit. (**C** and **D**) An ARS staining kit was performed to assess the osteoblast mineralization nodules. (**E**–**G**) The expression of OPN, BGLAP and RUNX2 was measured by qPCR. *P < 0.05, **P < 0.01 and ***P < 0.001.

reported that promotion of osteogenic differentiation is effective in improving osteoporosis. For example, Zhang et al.[22] demonstrated that CARM1 promotes osteogenic differentiation and decreases the bone loss in osteoporosis model mice. In addition, some drugs, including metformin, improve osteoporosis by promoting osteogenic differentiation[23]. Notably, some studies have proved that some traditional Chinese medicine monomer components have great potential in the treatment of osteoporosis[24]. In this study, we used ISO to treat MC3T3 cells, and demonstrated that ISO significantly promoted osteogenic differentiation of MC3T3 cell. ISO is a compound mainly exists in angelica dahurica that has been proven to be an apoptosis promoter[9]. Moreover, ISO is an effective anti-inflammatory medicine that has been shown potential in the treatment of periodontitis[7]. However, the role of ISO in osteogenic differentiation has not been reported. A previous study demonstrated that ISO inhibited osteoclast generation and bone loss in OVX-induced rats, suggesting the potential of ISO on improving osteoporosis[12]. Based on this study mentioned above, we investigated the effect of ISO on osteogenic differentiation for the first time, and demonstrated that ISO alleviated osteoporosis in OVX mice. This study first indicated the good effect of ISO in the treatment of osteoporosis, indicating the potential of ISO as a medicine for the treatment of osteoporosis.

m5C modification is a widespread RNA methylation modification involved in cellular activities by regulating RNA stability. Studies on m5C mainly focus on its role in the progression of cancers. Numerous studies have shown that aberrant expression of the overall modification of m5C and its regulators, including "writers", "erasers" and "readers", mediates the development of cancer[25]. However, the regulatory role and mechanism of m5C modification in osteoporosis have not been reported. In this study, we demonstrated that ISO promoted the m5C modification and the expression of YBX1. YBX1 is a m5C reader, and current studies on its function have focused on its regulatory role in cancer[26,27]. Notably, the role of YBX1 in osteogenic differentiation has also been demonstrated in recent years, and YBX1 promotes osteogenesis and ameliorates bone loss in OVX mice in an m5C-dependent manner[20]. Moreover, deletion of YBX1 in BMSCs accelerated bone loss in mice, while its overexpression stimulated bone formation[28]. These results may demonstrate the role of YBX1 in promoting osteogenic differentiation. Similarly to previous studies, we confirmed that YBX1 knockdown inhibited osteogenic differentiation in ISO-treated MC3T3 cells, as well as restored the osteoporosis in improved by ISO in OVX-induced mice. In summary, our study not only confirmed the promoting effect of YBX1 on osteogenic

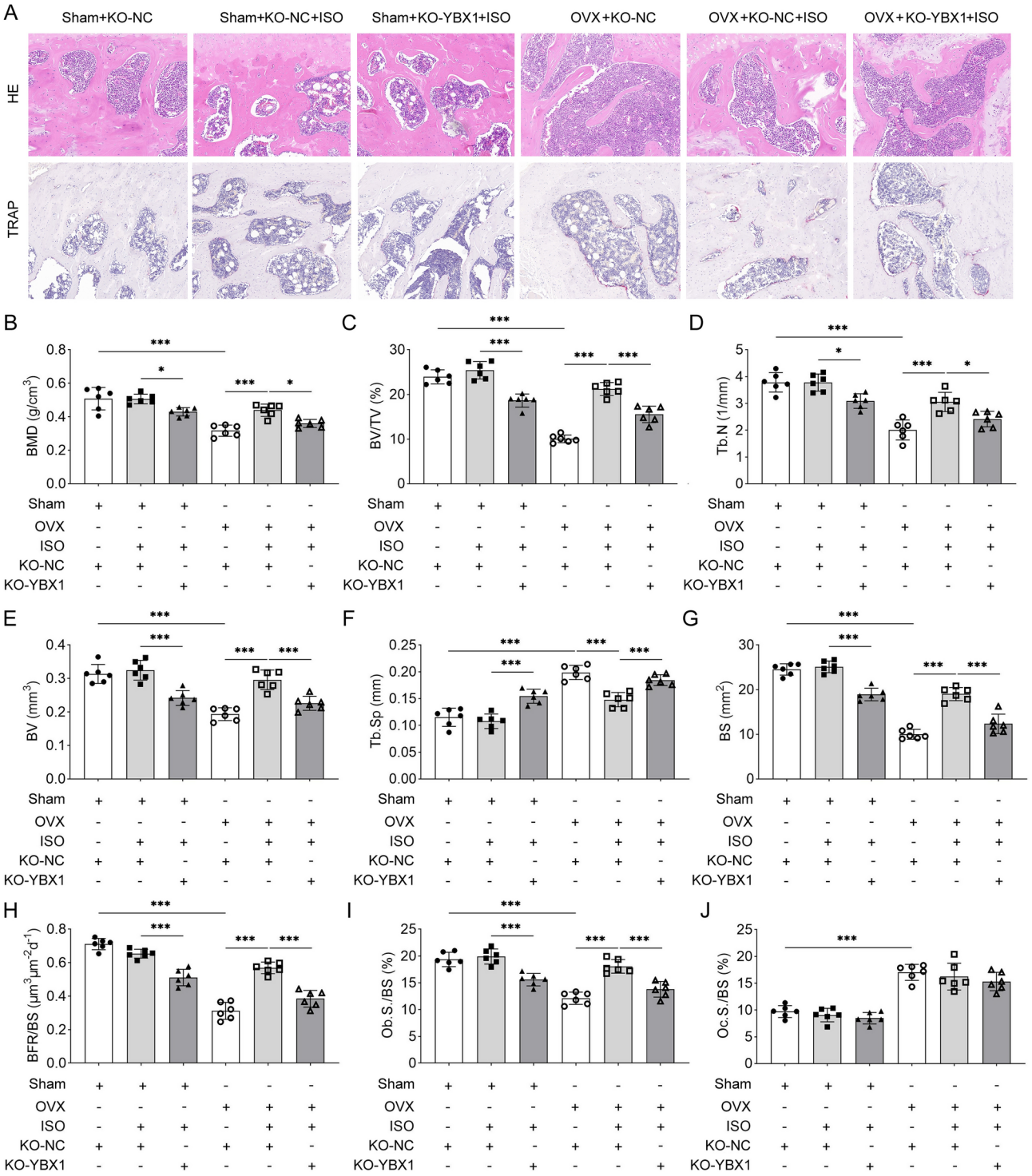

Fig. 5. YBX1 knockdown reversed the osteoporosis in OVX mice alleviated by ISO. (**A**) The pathological change and osteoclastic differentiation of different group mice was assessed by H&E and TRAP staining. (**B**–**G**) BMD, BV/TV, Tb.N, BV, Tp.Sp and BS were detected by microCT. (**H**) BFR/BS was measured by dynamic histomorphometry. (**I**) Ob.S./BS was evaluated by H&E staining (**J**) Oc.S./BS were evaluated by TRAS staining. *P < 0.05 and ***P < 0.001.

differentiation and its beneficial role in osteoporosis but also, for the first time, identified YBX1 as a regulatory target of ISO in osteoporosis. These findings revealed the mechanism of ISO ameliorated osteoporosis through m5C modification.

Additionally, we demonstrated that YBX1 knockdown inhibited the m5C modification level of BGLAP through suppressing it RNA stability. BGLAP, also known as osteocalcin, is a regulator of osteogenic differentiation

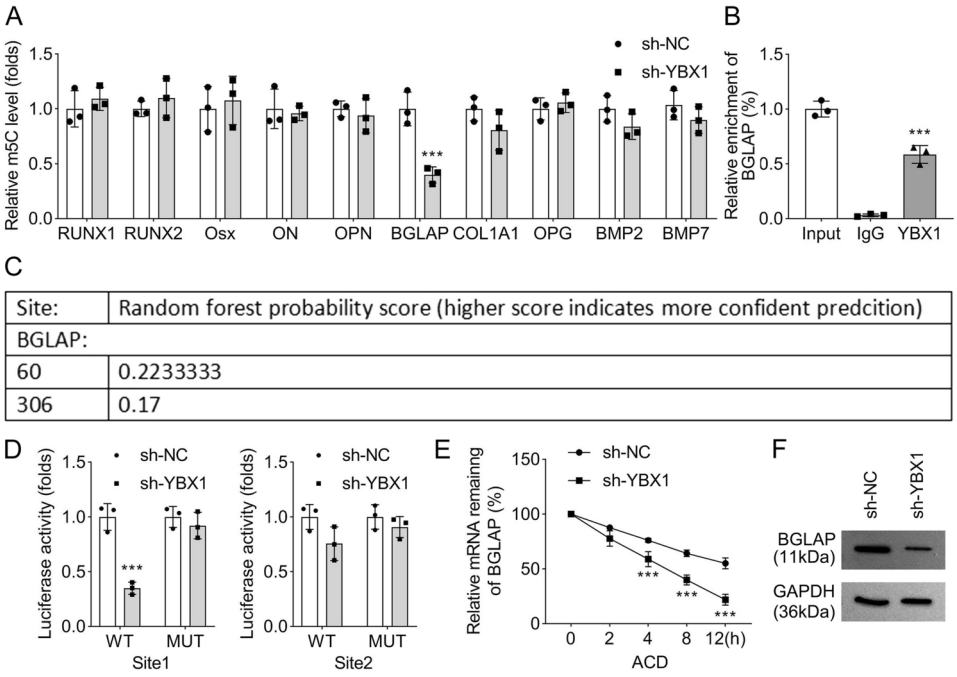

Fig. 6. YBX1 knockdown inhibited the m5C level of BGLAP. (**A**) The m5C levels of osteogenesis-related genes was measured using a m5C MeRIP kit. (**B**) The interaction between BGLAP and YBX1 was identified by RIP. (**C**) The potential m5C sites were predicted by RNAm5Cfinder database. (**D**) Dual luciferase reports were performed to identify BGLAP m5C site. (**E**) qPCR was performed to measure the expression BGLAP in MC3T3 cells after treatment of 5 μg/mL actinomycin D for 0, 2, 4 and 8 h. (**F**) The protein levels of BGLAP in MC3T3 cells were detected by western blot. ***P < 0.001 vs. the sh-NC group or input group.

and a key regulatory gene in osteoporosis. Liu et al.[29] demonstrated that BGLAP expression and osteogenic differentiation is decreased in aged mice. Yoshida et al.[30] revealed that RUBCN deficiency in osteoblasts leads to the increase of BGLAP expression thereby promoting osteoblast differentiation and alleviating osteoporosis. Additionally, Zhang et al.[31] confirmed that the expression of BGLAP is downregulated in mesenchymal stem cells of mice. In this study, we firstly investigated the m5C modification on BGLAP, and revealed that YBX1 knockdown inhibited the m5C level of BGLAP through inhibiting its RNA stability, suggesting that YBX1 mediated osteoporosis through regulating the level of BGLAP m5C modification. Moreover, we demonstrated that the m5C modification site of BGLAP was site 60. The identification of m5C sites in BGLAP RNA provides insights into the regulatory mechanisms governing BGLAP expression and function. The m5C modifications were primarily found in the 5' UTR and coding region of the BGLAP transcript. These regions are known to play crucial roles in mRNA stability, translation efficiency, and splicing regulation. the m5C modifications in BGLAP RNA represent a novel layer of epigenetic regulation that modulates BGLAP expression and function. Understanding the specific roles of these m5C sites could provide new targets for therapeutic interventions in bone-related diseases.

In conclusion, we revealed for the first time the mechanism of ISO in treating osteoporosis through m5C modification, and confirmed that ISO improved osteoporosis by elevating YBX1 expression to increase the level of BGLAP m5C modification. These findings not only provide a novel theoretical basis for understanding the mechanism of ISO in the treatment of osteoporosis but also open new avenues for the development of targeted therapies. By uncovering the role of m5C modification and YBX1 in osteogenic differentiation, our research contributes significantly to the field of bone biology and offers promising insights for the prevention and treatment of osteoporosis.

Data availability

The datasets used and/or analysed during the current study are available from the corresponding author on reasonable request.

Received: 5 August 2024; Accepted: 12 March 2025
Published online: 21 March 2025

References

1. Qaseem, A. et al. Pharmacologic treatment of primary osteoporosis or low bone mass to prevent fractures in adults: a living clinical guideline from the American College Of Physicians. *Ann. Intern. Med.* **176**, 224–238 (2023).
2. Skowrońska-Jóźwiak, E. & Lewandowski, K. Editorial: osteoporosis secondary to endocrine disorders. *Front. Endocrinol. Lausanne* **14**, 1194241 (2023).

3. Jiang, Y., Zhang, P., Zhang, X., Lv, L. & Zhou, Y. Advances in mesenchymal stem cell transplantation for the treatment of osteoporosis. *Cell Proliferat.* **54**, e12956 (2021).
4. Wright, N. C. et al. The recent prevalence of osteoporosis and low bone mass in the united states based on bone mineral density at the femoral neck or lumbar spine. *J. Bone Miner. Res.* **29**, 2520–2526 (2014).
5. Noh, J., Yang, Y. & Jung, H. Molecular mechanisms and emerging therapeutics for osteoporosis. *Int. J. Mol. Sci.* **21**, 7623 (2020).
6. Aibar-Almazán, A. et al. Current status of the diagnosis and management of osteoporosis. *Int. J. Mol. Sci.* **23**, 9465 (2022).
7. Fan, L., Li, Z., Gao, L., Zhang, N. & Chang, W. Isoimperatorin alleviates lipopolysaccharide-induced periodontitis by downregulating Erk1/2 and Nf-Kb pathways. *Open Life Sci.* **18**, 20220541 (2023).
8. Rajendran, P., Althumairy, D., Bani-Ismail, M., Bekhet, G. M. & Ahmed, E. A. Isoimperatorin therapeutic effect against aluminum induced neurotoxicity in albino mice. *Front. Pharmacol.* **14**, 1103940 (2023).
9. Tong, K., Xin, C. & Chen, W. Isoimperatorin induces apoptosis of the Sgc-7901 human gastric cancer cell line via the mitochondria-mediated pathway. *Oncol. Lett.* **13**, 518–524 (2017).
10. Lai, Y. et al. Antiviral activity of isoimperatorin against influenza a virus in vitro and its inhibition of neuraminidase. *Front. Pharmacol.* **12**, 657826 (2021).
11. Yang, H. B. et al. Effects of isoimperatorin on proliferation and apoptosis of human gastric carcinoma cells. *Oncol. Lett.* **15**, 7993–7998 (2018).
12. Li, H. et al. Isoimperatorin attenuates bone loss by inhibiting the binding of rankl to rank. *Biochem. Pharmacol.* **211**, 115502 (2023).
13. Cui, L. et al. Rna modifications: importance in immune cell biology and related diseases. *Signal Transduct. Ther.* **7**, 334 (2022).
14. Zhou, Y. et al. Principles of Rna methylation and their implications for biology and medicine. *Biomed. Pharmacother.* **131**, 110731 (2020).
15. Li, M. et al. 5-Methylcytosine Rna methyltransferases and their potential roles in cancer. *J. Transl. Med.* **20**, 214 (2022).
16. Zhu, W. et al. Positive epigenetic regulation loop between Ar and Nsun2 promotes prostate cancer progression. *Clin. Transl. Med.* **12**, e1028 (2022).
17. Fang, L. et al. M5C-methylated Lncrna Nr_033928 promotes gastric cancer proliferation by stabilizing Gls Mrna to promote glutamine metabolism reprogramming. *Cell Death Dis.* **14**, 520 (2023).
18. Guo, G. et al. Disease activity-associated alteration of Mrna M5 C methylation in Cd4+ T cells of systemic lupus erythematosus. *Front. Cell Dev. Biol.* **8**, 430 (2020).
19. Song, Y. et al. Comprehensive analysis of key M5C modification-related genes in type 2 diabetes. *Front. Genet.* **13**, 1015879 (2022).
20. Li, Y. et al. Ybx1 promotes type H vessel-dependent bone formation in an M5C-dependent manner. *JCI insight.* **9**, 4 (2024).
21. Verdonck, C., Willems, R. & Borgermans, L. Implementation and operationalization of integrated people-centred health services delivery strategies in integrated osteoporosis care (Ioc) initiatives: a systematic review. *Osteoporosis Int.* **34**, 841–865 (2023).
22. Zhang, L. et al. Arginine methylation of Ppp1Ca by Carm1 regulates glucose metabolism and affects osteogenic differentiation and osteoclastic differentiation. *Clin. Transl. Med.* **13**, e1369 (2023).
23. Zheng, L. et al. Metformin promotes osteogenic differentiation and prevents hyperglycaemia-induced osteoporosis by suppressing ppargamma expression. *Acta Biochim. Biophys. Sin.* **55**, 394–403 (2023).
24. Zhuo, Y. et al. Evolving roles of natural terpenoids from traditional Chinese medicine in the treatment of osteoporosis. *Front. Endocrinol.* **13**, 901545 (2022).
25. Chen, Y. et al. 5-methylcytosine transferase Nsun2 drives Nrf2-mediated ferroptosis resistance in non-small cell lung cancer. *J. Biol. Chem.* **2024**, 106793 (2024).
26. Liu, X. et al. Rna M5C modification upregulates E2F1 expression in a manner dependent on Ybx1 phase separation and promotes tumor progression in ovarian cancer. *Exp. Mol. Med.* **56**, 600–615 (2024).
27. Yu, T. et al. Thoc3 interacts with Ybx1 to promote lung squamous cell carcinoma progression through Pfkfb4 Mrna modification. *Cell Death Dis.* **14**, 475 (2023).
28. Xiao, Y. et al. Splicing factor Ybx1 regulates bone marrow stromal cell fate during aging. *EMBO J.* **42**, e111762 (2023).
29. Liu, Z. et al. Autophagy receptor optn (optineurin) regulates mesenchymal stem cell fate and bone-fat balance during aging by clearing Fabp3. *Autophagy* **17**, 2766–2782 (2021).
30. Yoshida, G. et al. Degradation of the notch intracellular domain by elevated autophagy in osteoblasts promotes osteoblast differentiation and alleviates osteoporosis. *Autophagy* **18**, 2323–2332 (2022).
31. Zhang, K. et al. Macf1 overexpression in Bmscs alleviates senile osteoporosis in mice through Tcf4/Mir-335–5P signaling pathway. *J. Orthop. Transl.* **39**, 177–190 (2023).

Author contributions

All authors participated in the design, interpretation of the studies and analysis of the data and review of the manuscript. G H and J W drafted the work and revised it critically for important intellectual content; H Y was responsible for the acquisition, analysis and interpretation of data for the work; G H and K Z made substantial contributions to the conception or design of the work. All authors read and approved the final manuscript.

Funding

The work was supported by Guizhou health and Health Committee(gzwkj2023-178).

Competing interests

The authors declare no competing interests.

Ethics approval and consent to participate

This study was approved by the Ethics Committee of The First Affiliated Hospital of Guizhou University of Traditional Chinese Medicine.All animal experiments should comply with the ARRIVE guidelines.All methods were carried out in accordance with relevant guidelines and regulations.

Additional information

Correspondence and requests for materials should be addressed to K.Z.